IEEE Access
Multidisciplinary | Rapid Review | Open Access Journal

Received June 29, 2020, accepted July 5, 2020, date of publication July 13, 2020, date of current version July 23, 2020.

Digital Object Identifier 10.1109/ACCESS.2020.3008883

BER-Adaptive RMLSA Algorithm for Wide-Area Flexible Optical Networks

FELIPE IGNACIO CALDERÓN[1], ASTRID LOZADA[2], DANILO BÓRQUEZ-PAREDES[3], RICARDO OLIVARES[2], ENRIQUE JAVIER DAVALOS[4], (Member, IEEE), GABRIEL SAAVEDRA[5], (Member, IEEE), NICOLÁS JARA[2], AND ARIEL LEIVA[1], (Member, IEEE)

[1]School of Electrical Engineering, Pontificia Universidad Católica de Valparaíso, Valparaíso 2362804, Chile
[2]Department of Electronic Engineering, Universidad Técnica Federico Santa María, Valparaíso 2390123, Chile
[3]Faculty of Engineering and Science, Universidad Adolfo Ibáñez, Santiago 7941169, Chile
[4]Polytechnical Faculty, Universidad Nacional de Asunción, San Lorenzo 2111, Paraguay
[5]Electrical Engineering Department, Universidad de Concepción, Concepción 4070409, Chile

Corresponding author: Ariel Leiva (ariel.leiva@pucv.cl)

This work was supported in part by under Grant DI-PUCV 039.437, in part by under Grant USM PI LII_2020_74, and in part by Agencia Nacional de Investigación y Desarrollo de Chile (ANID) FONDECYT Iniciación under Grant 11190710.

ABSTRACT Wide-area optical networks face significant transmission challenges due to the relentless growth of bandwidth demands experienced nowadays. Network operators must consider the relationship between modulation format and maximum reach for each connection request due to the accumulation of physical layer impairments in optical fiber links, to guarantee a minimum quality of service (QoS) and quality of transmission (QoT) to all connection requests. In this work, we present a BER-adaptive solution to solve the routing, modulation format, and spectrum assignment (RMLSA) problem for wide-area elastic optical networks. Our main goal is to maximize successful connection requests in wide-area networks while choosing modulation formats with the highest efficiency possible. Consequently, our technique uses an adaptive bit-error-rate (BER) threshold to achieve communication with the best QoT in the most efficient manner, using the strictest BER value and the modulation format with the smallest bandwidth possible. Additionally, the proposed algorithm relies on 3R regeneration devices to enable long-distances communications if transparent communication cannot be achieved. We assessed our method through simulations for various network conditions, such as the number of regenerators per node, traffic load per user, and BER threshold values. In a scenario without regenerators, the BER-Adaptive algorithm performs similarly to the most relaxed fixed BER threshold studied in blocking probability. However, it ensures a higher QoT to most of the connection requests. The proposed algorithm thrives with the use of regenerators, showing the best performance among the studied solutions, enabling long-distance communications with a high QoT and low blocking probability.

INDEX TERMS Elastic optical networks, routing, modulation level, spectrum allocation, bit error rate, quality of service.

I. INTRODUCTION

The bandwidth demand over telecommunication networks has increased explosively over time, with average increases of approximately 30% per year [1]. So far, optical network infrastructures have been able to support the increasing traffic demands. However, several studies have anticipated a potential ''capacity crunch'' on current networks [2], [3], arising from the limits imposed by Kerr non-linearity. Therefore, a potential inability to support future traffic demands will be reached shortly.

One course of action to overcome this problem is to manage the installed network infrastructure efficiently [4], [5]. Nowadays, signals are multiplexed and transmitted using different carrier frequencies/wavelengths within a pre-established grid (50 or 100 GHz separation per channel) [6]. To satisfy the growth in traffic demand, Internet Service Providers are increasing the user bit-rates within this fixed

The associate editor coordinating the review of this manuscript and approving it for publication was Muhammad Omer Farooq.

transmission grid, relying on complex modulation formats, higher symbol rates, or both [4].

To overcome this scenario, a new architecture was proposed during the last decade called ''Elastic Optical Networks'' (EON) [1], [7]. EON assign the frequency spectrum to different users based on their bandwidth requirements. The spectrum is divided into subsections of 12.5 GHz called ''frequency slot units'' (FSUs), which can be grouped flexibly to provide sufficient spectrum for each user according to their needs. This way, flexible operation may minimize idle bandwidth and serve a greater number of users, compared to a fixed grid.

One of the main tasks operators of EON must solve is to assign a path and a portion of the spectrum to each connection request. This problem is known as the ''routing and spectrum assignment'' (RSA) problem. In wide-area networks, such as continental networks, the problem becomes more complex, since the relationship between modulation format and a maximum reach for each connection request must be considered. This problem is known as the ''routing, modulation level, and spectrum assignment'' (RMLSA) problem. Then, for a given transmission request, the RMLSA problem consists on finding a path, a modulation format suitable for the path length, and a portion of the optical spectrum on the path (measured as the number of FSUs) [8]–[16]. The connections are only achievable if an acceptable quality of transmission (QoT) is obtained after transmission considering the physical layer impairments (PLI) accumulated during propagation. In optical fiber links, amplified spontaneous emission (ASE) noise and non-linear distortions accumulate over distance and, in practice, cannot be entirely compensated for. RMLSA solutions must ensure both an acceptable blocking probability, that measures the chance that a given user may not transmit due to a lack of resources, and a minimum QoT for each user request. Thus, a given transmission request succeeds if enough resources are available on the selected path, and the QoT threshold is not exceeded; else, the request is rejected.

Standard approaches to solve the RMLSA problem establish end-to-end all-optical communication (i.e., transparent) between source-destination node pairs [10]–[17]. However, the accumulation of PLI limits the generation of transparent connections in wide-area elastic optical networks. Several users may not achieve transparent communication through long distances despite the modulation format chosen. Therefore, the use of 3R (Re-amplification, Re-shaping, and Re-timing) regeneration in wide-area elastic optical networks cannot be avoided. Besides, due to the relentless growth of bandwidth demands, some communications must use highly efficient modulation formats to avoid excessive use of frequency slots. However, these modulation formats have low noise tolerance, strengthening the need to consider regeneration devices on the RMLSA approaches.

In this context, different RMLSA algorithms approaches have been proposed in the literature using 3R regeneration. In [18], the authors present an RMLSA scheme using regenerators that minimizes the network energy consumption and reduces the blocking probability of the users. They achieve these goals ensuring a predefined BER threshold, calculated using a physical layer model that includes both ASE noise and non-linear phenomena [19]. In [20], the authors consider energy efficiency parameters in the resource assignment procedures but only use ASE noise in the physical layer with a fixed BER threshold value of 10^{-9}. Authors of [21] present an adaptive routing algorithm using a cost function to choose the path and regeneration nodes, considering link usage metrics and penalizing the use of regenerators. Nevertheless, the computation overhead of an adaptive routing strategy is significantly higher than the fixed or fixed-alternate solutions.

RMLSA algorithms considering 3R regeneration devices use regenerators assignment policies to choose in which node along the user path the 3R regeneration is going to take place. Authors of [22], [23] formulate two regenerator assignment policies denoted as FLR (First Longest Reach Regenerator) and FNS (First Narrowest Spectrum Regenerator). The first one establishes the longest reach transparent segment-first, regenerating as far away from the source node as possible. The second one also establishes the longest transparent segment, but with the most efficient modulation format. In [24], [25] the authors propose CIRA (Circuit Invigorating Regenerator Assignment), which is a variation of FLR, establishing a connection based on the spectrum availability on the candidate route and the detrimental effect due to PLI..

The described solutions of the RMLSA problem rely on a predefined BER threshold to establish or reject a given communication request. The BER thresholds define if a transmission has an acceptable quality, and, at the same time, they determine the maximum reach for a modulation format - bit rate pair. Accordingly, an optical connection request can be accepted or rejected depending on this parameter. In general, for wide-area optical networks, a permissive BER threshold leads to a low rate of blocking transmission requests due to optical reach, and a strict BER threshold decreases the capability to achieve long-distance communications. Notwithstanding, both BER threshold criteria allow for successful transmissions, but with different signal quality which may be corrected at the receiver to some extent. One of the primary goals in optical communications is to successfully accomplish transmission requests. Consequently, a fixed BER threshold value may not be enough to maximize communications in wide-area networks.

In this work, we propose a BER-adaptive RMLSA algorithm to manage wide-area elastic optical networks efficiently. The main motivation is to enable long distance transmissions with a high QoT using an spectrally efficient modulation format. This is achieved customizing the BER thresholds in an adaptive manner, and using one regenerator device per connection request, if necessary. For each connection request the algorithm prioritizes to reach the destination with the best BER possible, and secondly, it chooses the most efficient modulation level in terms of capacity demanded.

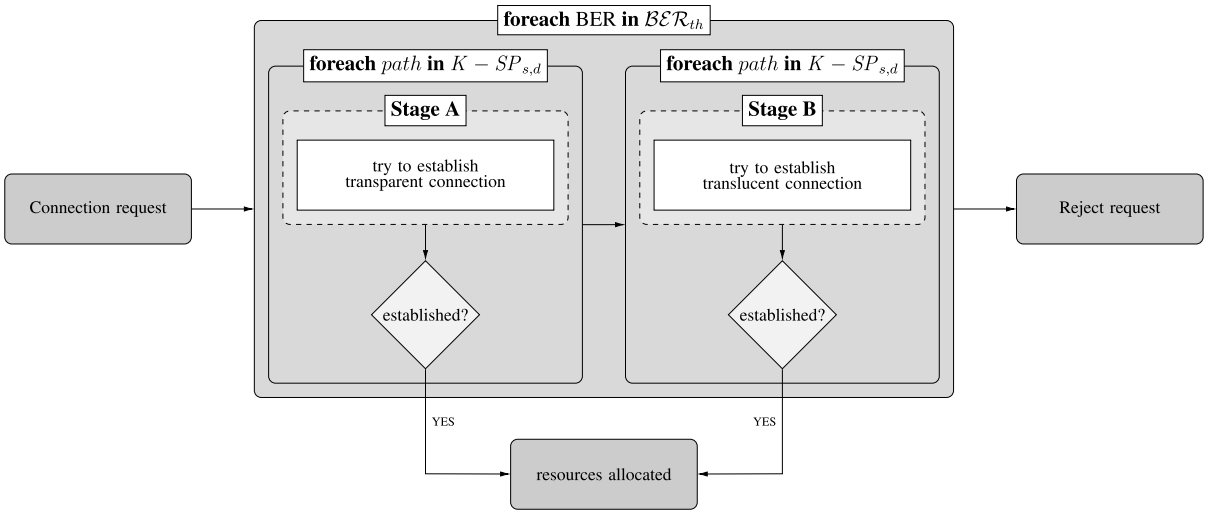

FIGURE 1. BER-Adaptive RMLSA flow chart.

In this way, we maximize the transmission acceptance rate, while using the minimum amount of FSUs, and with the best (most strict/lowest) BER value possible.

The remainder of this paper is structured as follows: Section II presents our proposal to solve the RMLSA problem. In Section III, we display the physical layer model and network simulation tools used to assess the performance of the proposed algorithm. Next, Section IV contains numerical examples of the proposed algorithm. Finally, we provide some conclusions and remarks in Section V.

II. BER-ADAPTIVE RMLSA STRATEGY

In this section, the used network and traffic models and the associated assumptions are presented. Then, the definitions used within the algorithms are described, and finally, the proposed algorithm to solve the RMLSA problem is presented.

A. NETWORK AND TRAFFIC MODEL

The graph $\mathcal{G} = (\mathcal{N}, \mathcal{E})$ represents the network topology, where $\mathcal{N}$ is the set of network nodes, and $\mathcal{E}$ is the set of unidirectional links (the arcs in $\mathcal{G}$). The set of users $\mathcal{X}$ is composed by all the source-destination pairs (s, d) with communication between them.

We use an ON-OFF model to represent the traffic between a given source-destination pair. Consider user (s, d). During any of its ON periods, with average length $t_{ON(s,d)}$, the source transmits at a constant rate. During an OFF period, with average length $t_{OFF(s,d)}$, the source refrains from transmitting data.

The used technology determines the constant transmission rate during the ON periods, but to simplify the presentation, the rate was set to unity. Consequently, the traffic load of a user (s, d), denoted by $\varrho_{(s,d)}$, is given by:

$$\varrho_{(s,d)} = \frac{t_{ON(s,d)}}{t_{ON(s,d)} + t_{OFF(s,d)}}. \quad (1)$$

In this work we consider the case where the load is equal for all users, the so called homogeneous situation.

B. BER-ADAPTIVE RMLSA ALGORITHM

The main steps of our BER-Adaptive RMLSA solution are illustrated in Figure 1 and explained on the pseudo-code presented in Algorithm 1. The definitions required for the explanation of the algorithm are presented in the following list:

- $B_{s,d}$ is the bit-rate required by the connection between s and d;
- The set $\mathcal{BER}_{th} = \left\{BER^1_{th}, \ldots BER^e_{th}, \ldots BER^E_{th}\right\}$ is composed of the BER threshold considered to establish optical connections. The elements are ordered from most strict BER to the most relaxed one. The cardinality of this set is E;
- The set $\beta = \left\{B^1, B^2, \ldots B^u, \ldots B^U\right\}$ is composed of the transmission rates available at the flexible transponders. The parameter B^u denotes the u-th bit-rate available on the set;
- The set $\mathcal{M} = \left\{M^1, M^2, \ldots M^j, \ldots M^J\right\}$ contains the J modulation formats available on the flexible transponders. The element M^j denotes the j-th modulation format on the set;
- The set $\mathcal{P}_{s,d} = \left\{P^1_{s,d}, P^2_{s,d}, \ldots P^k_{s,d}, \ldots P^K_{s,d}\right\}$ is composed of the K candidate paths between the nodes s and d. The $P^k_{s,d}$ element denotes the k-th shortest route. These paths can be pre-computed using any method available in the literature (for instance, [26]);
- The set $\mathcal{L}_{s,d} = \left\{L^1_{s,d}, L^2_{s,d}, \ldots L^k_{s,d}, \ldots L^K_{s,d}\right\}$ is composed of the path lengths of the user (s, d), in kilometers (km), in which $L^k_{s,d}$ is the length of the k-th route of a user (s, d) $(P^k_{s,d})$;
- Let C be the link capacity in terms of FSUs.
- The matrix $\mathbb{FSU}(\mathcal{A}, \mathcal{D})$ is composed by the elements $\mathbb{FSU}[m, b]$, and stores the number of FSUs required

for a modulation format m and a transmission rate b, $\forall m \in \mathcal{A} \subseteq \mathcal{M}$ and $b \in \mathcal{D} \subseteq \beta$.

- The procedure $\mathcal{FM}(L_{s,d}, B_{s,d}, BER^{e}_{th})$ computes a list of modulation formats with an optical reach equal or higher than $L_{s,d}$, considering the bit-rate $B_{s,d}$, and the BER threshold BER^{e}_{th}.

The proposed algorithm works as follows: Upon receiving a connection request between nodes s and d, with a bit-rate of $B_{s,d}$, the algorithm searches for the available capacity to transmit in the candidate paths using the most strict BER threshold first (line **1**). The first inner loop (line **2 to 7**) attempts to allocate a transparent connection in one of the K different paths in the set $\mathcal{P}_{s,d}$. If a transparent connection is not allocated, then the second loop (lines **8 to 13**) follows an identical process but using one regeneration device per path. If a connection request could not be assigned in any loop, then the algorithm repeats the process considering the next BER threshold on the list.

Algorithm 1 BER-Adaptive RMLSA Algorithm

Require: $s, d, B_{s,d}, \mathcal{BER}_{th}, \mathcal{L}_{s,d}, \mathcal{P}_{s,d}, K, C$.

1: **for** $\{e \in \mathbb{Z}^{+} : e \leq E\}$ **do**
2: **for** $\{k \in \mathbb{Z}^{+} : k \leq K\}$ **do**
3: $rtn_A = Stage\_A(L^{k}_{s,d}, B_{s,d}, BER^{e}_{th}, P^{k}_{s,d}, C)$
4: **if** $rtn_A = successful$ **then**
5: **return** *resources allocated*
6: **end if**
7: **end for**
8: **for** $\{k \in \mathbb{Z}^{+} : k \leq K\}$ **do**
9: $rtn_B = Stage\_B(L^{k}_{s,d}, B_{s,d}, BER^{e}_{th}, P^{k}_{s,d}, C)$
10: **if** $rtn_B = successful$ **then**
11: **return** *resources allocated*
12: **end if**
13: **end for**
14: **end for**
15: **return** *reject request*

Lines **3** and **9** show the two sub-procedures *Stage_A* and *Stage_B*, which are explained in detail next.

Stage A: In this stage, the feasibility of establishing a transparent connection is evaluated considering a given BER threshold value BER_{th}. In this stage the modulation format that requires the lowest number of FSUs, and has an optical reach greater than or equal to the length of the selected path is chosen. Subsequently, the spectrum assignment (SA) procedure is executed. The SA problem has been widely covered in the literature [1], [27]. Among them, First-Fit is currently the most popular method, due to its good performance in terms of blocking probability with low computational complexity. As a consequence, First-Fit (denoted as *FF*) was used to allocate the FSUs, saving its return state in *rtn* variable. The FF procedure must comply with the known continuity and contiguity constraints. The continuity constraint states that the FSUs assigned to one connection must be maintained along the entire origin-destination path. On the other hand, the contiguity constraint states that, if the user bandwidth requirements must be satisfied with more than one FSU, they must be contiguous in the spectrum.

Symbolically we evaluate this stage by writing *Stage_A*(), displayed as a pseudo-code in Algorithm 2.

Algorithm 2 Stage a

Require: $L_{s,d}, B_{s,d}, BER_{th}, P_{s,d}, C$.

1: $\mathcal{A} = \mathcal{FM}(L_{s,d}, B_{s,d}, BER_{th})$
2: **if** $\mathcal{A} \neq \emptyset$ **then**
3: $n = \min(\mathbb{FSU}(\mathcal{A}, \{B_{s,d}\}))$
4: $rtn = FF(P_{s,d}, n, C)$
5: **if** $rtn = successful$ **then**
6: **return** *successful*
7: **else**
8: **return** *Non-successful*
9: **end if**
10: **else**
11: **return** *Non-successful*
12: **end if**

For a path $P_{s,d}$, in line **1**, the algorithm calculates the set of the modulation formats $\mathcal{A}$ complying with the required optical reach for transparent communication considering a specific BER threshold value. If this set has at least one element, then the modulation format requiring the lowest number of FSUs is selected (line **3**). Next, the spectrum allocation algorithm (*FF*) is executed to find a set of contiguous and continuous FSUs on the links belonging to the analyzed path. If the FF algorithm finds a solution, then the process returns *successful* (value of variable rtn_A in line **3** of Algorithm 1), and the resources are reserved, and the connection is established. Otherwise, the process returns *Non successful*.

Stage B: This stage is executed when it is not possible to establish a transparent connection between node s and d through any path in $\mathcal{P}_{s,d}$ considering a specific value of BER threshold. In this case, the algorithm divides the path into 2 sub-paths, with a regeneration device in the node between them. To understand stage B, some additional definitions are described as follows:

- Let $N(P_{s,d})$ be the number of nodes in route $P_{s,d}$.
- Let $\Omega(N_i)$ be the number of conversion/regeneration devices available at the node N_i of the path $P_{s,d}$ in a given time.
- Let $\mathcal{S}(P_{s,d}) = \{S^1(P_{s,d}), \ldots, S^i(P_{s,d}), \ldots\ldots, S^{N(P_{s,d})-2}(P_{s,d})\}$ be the set of segments in path $P_{s,d}$, such that segment $S^i(P_{s,d})$ originates at the source node s of path $P_{s,d}$, and ends at the i-th node previous to node d along the path. Figure 2 shows an example of a path (P_{AD}) consisting of 4 nodes between nodes A and D. In this case, the set $\mathcal{S}(P_{AD})$ has two elements: segments $\mathcal{S}^1(P_{AD})$ and $\mathcal{S}^2(P_{AD})$.
- Let $\mathcal{S}(P_{s,d})^* = \{S^1(P_{s,d})^*, \ldots, S^i(P_{s,d})^*, \ldots\ldots, S^{N(P_{s,d})-2}(P_{s,d})^*\}$ be the set of segments in $P_{s,d}$ such that segment $S^i(P_{s,d})^*$ starts at the i-th node previous to destination node d and ends at node d. Figure 2

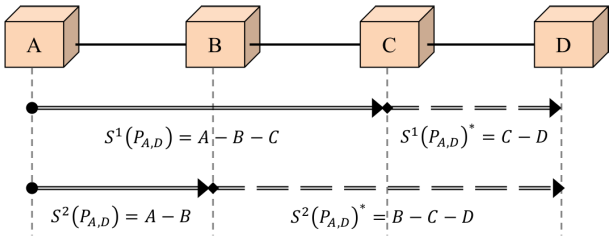

FIGURE 2. Set of segments associated with a 4-node path.

shows these segments for the 4-node path between nodes A and D.

- Let $L[S^i(P_{s,d})]$ and $L[S^i(P_{s,d})^*]$ be the length, in km, of segments $S^i(P_{s,d})$ and $S^i(P_{s,d})^*$, respectively.
- Let $\mathcal{FM}(L[S^i(P_{s,d})], B_{s,d}, BER_{th})$ and $\mathcal{FM}(L[S^i(P_{s,d})^*), B_{s,d}, BER_{th}]$ be the sets of modulation formats in $\mathcal{M}$ that, along with the bit rate $B_{s,d} \in \beta$, have an optical reach equal to or higher than $L[S^i(P_{s,d})]$ and $L[S^i(P_{s,d})^*]$, respectively, considering a specific value BER_{th} by bit error rate.

Symbolically we call Stage B by writing *Stage_B*(), shown as a pseudo-code in Algorithm 3.

Algorithm 3 Stage B

Require: $L_{s,d}, B_{s,d}, BER_{th}, P_{s,d}, C$.
1: **for** $\{i \in \mathbb{Z}^+ : i \leq N(P_{s,d}) - 2\}$ **do**
2: **if** $\Omega(N_i) \neq 0$ **then**
3: $\mathcal{A} = \mathcal{FM}(L[S^i(P_{s,d})], B_{s,d}, BER_{th})$
4: **if** $\mathcal{A} = \emptyset$ **then**
5: **return** *Non-successful*
6: **end if**
7: $n_1 = \min(\mathbb{FSU}(\mathcal{A}, \{B_{s,d}\}))$
8: $rtn_1 = FF(S^i(P_{s,d}), n_1, C)$
9: **if** $rtn_1 = successful$ **then**
10: $\mathcal{A}^* = \mathcal{FM}(L[S^i(P_{s,d})^*], B_{s,d}, BER_{th})$
11: **if** $\mathcal{A}^* = \emptyset$ **then**
12: **return** *Non-successful*
13: **end if**
14: $n_2 = \min(\mathbb{FSU}(\mathcal{A}^*, \{B_{s,d}\}))$
15: $rtn_2 = FF(S^i(P_{s,d})^*, n_2, C)$
16: **if** $rtn_2 = successful$ **then**
17: **return** *successful*
18: **else**
19: *release resources*
20: **end if**
21: **end if**
22: **end if**
23: **end for**
24: **return** *Non-successful*

In this stage, path $P_{s,d}$ is divided into two segments (loop in lines **1 to 23**). If the node between both segments has generators available (line **2**), then the algorithm tries to allocate resources for the first segment (lines **3 to 8**). If the allocation is successful, then the resource assignment for the second segment is attempted (lines **9 to 15**). It is assumed that the regeneration device can convert the modulation format and change the spectral position, using the First-Fit spectrum allocation procedure. If the connection between s and d cannot be established using these two segments, stage B re-starts considering a different set of segments. This procedure is repeated until the connection can be established (in this case, the process return $rtn_B = successful$ in line **9** of Algorithm 1) or until all the segment combinations in the path have been unsuccessfully attempted ($rtn_B = Non\text{-}successful$ on line **9** of Algorithm 1). The regenerator allocation policy used is based on the First Longest Reach Regenerator (FLR) algorithm [24].

C. COMPUTATIONAL COMPLEXITY

The total time complexity of the BER-adaptive RMLSA algorithm is calculated in four parts: *FF* algorithm, stage A, stage B, and the external for loop in Algorithm 1.

The time complexity of the *FF* algorithm is given by the maximum number of links ℓ in a path, and the number of total FSU by link C. So time complexity of *FF* is $\mathcal{O}_{FF}(\ell \cdot C)$. Line **3** of Stage A depends on the number of modulation formats J and bit-rates $|\{B_{s,d}\}|$, having a complexity time of $\mathcal{O}(J \cdot |\{B_{s,d}\}|)$. However, in practice, and simplifying the analysis, $J \cdot |\{B_{s,d}\}|$ generally will be less than $\ell \cdot C$, so complexity time of stage A will be $\mathcal{O}_{Stage\_A} = \mathcal{O}_{FF} = \mathcal{O}_{Stage\_A}(\ell \cdot C)$. Finally, Stage B has a similar analysis to stage A, but it has an extra outer loop. Then time complexity of Stage B is $\mathcal{O}_{Stage\_B}(\ell \cdot \ell \cdot C) = \mathcal{O}_{Stage\_B}(\ell^2 \cdot C)$.

Total time complexity is given by cardinality of the set $\mathcal{BER}_{th}$, K-Shortest Path, and the stage B algorithm: $\mathcal{O}(E \cdot K \cdot \ell^2 \cdot C)$, whose parameters are the cardinality of the set composed by the BER thresholds E, the number of paths K, the maximum number of links in a path ℓ, and the number of FSU C.

III. PHYSICAL LAYER MODEL AND NETWORK SIMULATION

Network simulations were carried out to assess the performance of the proposed RMLSA algorithm. The input for the network simulations is a set of the maximum achievable reach (MAR) for each modulation format - bit rate pair available in the transponders for every BER threshold in the $\mathcal{BER}_{th}$ set. To calculate the maximum reach for each modulation format and BER combinations, the GN model was used to estimate a received signal-to-noise ratio after transmission [28], [29].

In this article, we consider a coherent lightwave system transmitting information using a single polarization, where chromatic dispersion and polarization mode dispersion are ideally compensated for using digital signal processing. Additionally, cross-phase modulation and self-phase modulation are the principal non-linear effects. Furthermore, we assume that all components are carefully designed to avoid any additional source of noise, signal degradation, and crosstalk. For this system, the received SNR was used as a

performance metric and was calculated using:

$$SNR = \frac{p_{in}}{\eta_{ASE} + \eta_{NLI}}, \tag{2}$$

where p_{in} is the average input power, η_{ASE} is the ASE noise power, and η_{NLI} is the non-linear interference (NLI) noise power. For an amplification scheme based on erbium-doped fiber amplifiers (EDFAs), where links are made up of identical spans, and the loss of each span is exactly compensated by EDFAs, the total ASE noise power over a single polarization at the receiver is given by [30]:

$$\eta_{ASE} = \frac{1}{2} F_{EDFA} N_s h v A_{span} B_{ch}, \tag{3}$$

where N_s is the number of spans in the link, F_{EDFA} is the amplifier noise figure in linear units, h is Planck's constant, v is the carrier frequency, B_{ch} is the channel bandwidth and $A_{span} = 10^{(\alpha L_{span})/10}$ are the transmission losses in one span.

The NLI noise power was estimated using the Gaussian noise (GN) model [28], [29]. The GN model describes non-linear propagation in dispersion uncompensated coherent transmission systems and assumes that fiber nonlinearities can be modeled as additive white Gaussian noise that combines incoherently with ASE noise. The non-linear interference noise power was estimated using [31]:

$$\eta_{NLI} = N_s p_{in}^3 \eta_{NLI_{ss}}, \tag{4}$$

where $\eta_{NLI_{ss}}$ is the NLI noise power in a single span given by [28] $\eta_{NLI_{ss}} = G_{NLI}(f) B_{ch}$. The term $G_{NLI}(f)$ is the NLI power spectral density [29]:

$$G_{NLI}(f) = 2\gamma^2 \int_{-\infty}^{\infty}\int_{-\infty}^{\infty} G_{Tx}(f_1) G_{Tx}(f_2) G_{Tx}(f_1 + f_2 - f) \times \left| \frac{1 - e^{-2\alpha L_{span}} e^{j4\pi^2 \beta_2 L (f_1 - f)(f_2 - f)}}{2\alpha - j4\pi^2 \beta_2 (f_1 - f)(f_2 - f)} \right|^2 df_1 df_2, \tag{5}$$

where γ is the fiber nonlinearity coefficient, β_2 is the group velocity dispersion coefficient, and $G_{Tx}(f)$ is the power spectral density of the overall WDM transmitted channels. For a detailed derivation Eq. 5 the reader is referred to [29, Sec. IV].

The fiber parameters used for the calculations of the maximum achievable reach used throughout this work are shown in Table 1. The used parameters correspond to a standard single mode fiber (SMF), compiling with the ITU-T G.652 recommendations [32].

For simplicity, we assume that the optical reference bandwidth is equal to the symbol rate. Under this assumption, and using a matched filter at the receiver, inter-symbol interference (ISI) remains absent, the relation between the SNR and the OSNR, using single-polarization, is given by [30] $OSNR = 1/2 \times SNR$.

At optimum launch power, the MAR is obtained. The MAR is defined as the maximum number of spans that can be transmitted for a BER threshold at optimum launch power. The SNR is related to BER; in general, higher SNR values allow for lower BER values. For example, quadrature phase-shift keying (QPSK) modulation has a low SNR requirement, which implies that a long transmission distance is possible. On the other hand, higher quadrature amplitude modulation (QAM) constellations can carry more traffic, but with higher SNR requirements, they reach shorter distances. Modulation formats considered here are BPSK, QPSK, 8-QAM, 16-QAM, 32-QAM, and 64-QAM, each with a BER threshold of 10^{-6}, 10^{-9}, and 10^{-12}. To estimate the required SNR to satisfy the BER thresholds the following relationship was used [33]:

$$BER_{\Lambda-PSK} = \frac{1}{2}\text{erfc}\left(\sqrt{\frac{SNR}{\lambda}\frac{\Delta_{ref}}{B_{ch}}}\right), \tag{6}$$

$$BER_{\Lambda-QAM} = \frac{1}{\lambda}\left(1 - \frac{1}{\sqrt{\Lambda}}\right) \cdot \text{erfc}\left(\sqrt{\frac{3\ SNR}{2(\Lambda - 1)}\frac{\Delta_{ref}}{B_{ch}}}\right), \tag{7}$$

where $BER_{\Lambda-PSK}$ and $BER_{\Lambda-QAM}$ represent the BER obtained using PSK and QAM, respectively, with a constellation of cardinality Λ. λ represents the bits encoded in each constellation symbol, such that $\Lambda = 2^{\lambda}$. From equations 6 and 7, the SNR was obtained using the inverse complementary error function for each modulation format. Table 2 presents the required OSNR to achieve the BER thresholds and the bit-rate carried by each modulation format on a WDM channel using a single FSU.

Finally, using the OSNR thresholds from Table 2, the MAR was obtained. The MAR for each modulation format is shown in Table 3. This maximum reach represents the distance constraint in the modulation level selection in the BER-adaptive RMLSA algorithm proposed.

TABLE 1. Fiber parameters for maximum reach calculation.

Parameter	Symbol	Value
Fiber parameters		
Attenuation Coefficient	α	0.22 dB/km
Chromatic Dispersion Coefficient	β_2	$-21.3\text{ps}^2\text{km}^{-1}$
Nonlinear coefficient	γ	$1.3\text{W}^{-1}\text{km}^{-1}$
Optical Reference Bandwidth	Δ_{ref}	12.5 GHz
Span length	L_{span}	80 km
Amplifier parameters		
Noise Figure	F_{EDFA}	5 dB
Signal parameters		
Carrier Frequency	v	193.5 THz
Channel bandwidth	B_{ch}	12.5 GHz

TABLE 2. Required OSNR for various modulation formats to achieve a certain quality of transmission.

Modulation Format	Bit-rate (Gbps)	Required OSNR (dB) $BER = 10^{-6}$	$BER = 10^{-9}$	$BER = 10^{-12}$
BPSK	12.5	7.5	9.5	10.5
QPSK	25	10.5	12.5	13.5
8-QAM	37.5	13.5	16	17
16-QAM	50	17	19	20.5
32-QAM	62.5	20	22	23.5
64-QAM	75	23	25	26.5

TABLE 3. Maximum achievable reach (MAR) for modulation formats and BERs under study for a used bandwidth of $C = 320$ FSUs.

Modulation Format	Maximum achievable reach (km)		
	$BER = 10^{-6}$	$BER = 10^{-9}$	$BER = 10^{-12}$
BPSK	5520	3440	2720
QPSK	2720	1680	1360
8-QAM	1360	720	560
16-QAM	560	320	240
32-QAM	240	160	80
64-QAM	80	80	0

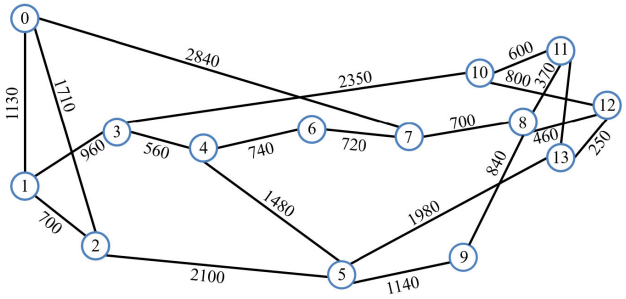

FIGURE 3. NSFnet network topology with the lengths of every optical link (in km).

IV. NUMERICAL EXAMPLES

In this section, we illustrate the performance of our BER-Adaptive proposal by comparing its output with several fixed BER thresholds approaches using 10^{-12}, 10^{-9}, and 10^{-6} values for their BER bounds on the NSFNet network topology (shown in Figure 3). Remark that, these BER values are standard bounds found in the literature [18], [19], [21].

The BER-adaptive RMLSA performance was evaluated using an event-discrete simulator based on C++. The simulation was made to represent how elastic optical networks behave, emulating the network operation and its technological restrictions. Each event on the simulator represents a connection request or release. Each connection requirement (defined by a source-destination pair and a bit rate) follows an ON-OFF traffic model. ON and OFF periods are exponentially distributed, with mean values denoted by t_{ON} and t_{OFF}, respectively. Observe that we address here the general case where the traffic load is assumed the same for all users, the so-called homogeneous situation.

All network users have different bit-rate demands, which are generated arbitrarily. The procedure chooses randomly between 10, 40, 100, 400, and 1000 Gbps values. Remark that we use the same seed in order to obtain the same random bit-rate requests. To translate the bit-rate demands to spectrum requirements, Table 4 illustrates the spectrum requirements in terms of the number of FSU and GHz for each bit-rate and modulation format combination. Then, for a given transmission request, the simulation computes the bandwidth demand based on the user bit-rate request and the best possible modulation format if the communication distance does not exceed the maximum achievable reach (MAR) displayed in Table 3.

TABLE 4. Spectrum requirements in terms of FSUs and GHz for each bit rate and modulation format pair.

Bit rate (Gbps)	Modulation format	Bandwidth (FSU)	Bandwidth (GHz)
10	BPSK	1	12.5
40	BPSK	4	50
40	QPSK	2	25
40	8-QAM	2	25
40	16-QAM	1	12.5
40	32-QAM	1	12.5
40	64-QAM	1	12.5
100	BPSK	8	100
100	QPSK	4	50
100	8-QAM	3	37.5
100	16-QAM	2	25
100	32-QAM	2	25
100	64-QAM	2	25
400	BPSK	32	400
400	QPSK	16	200
400	8-QAM	11	137.5
400	16-QAM	8	100
400	32-QAM	7	87.5
400	64-QAM	6	75
1000	BPSK	80	1000
1000	QPSK	40	500
1000	8-QAM	27	337.5
1000	16-QAM	20	250
1000	32-QAM	16	200
1000	64-QAM	14	175

We performed these simulations for different traffic loads, bit-rates, modulation formats, and the number of regenerators per node. Table 5 shows the values of the relevant parameters needed to perform the different simulation scenarios.

A. PERFORMANCE METRICS

The most critical metric on dynamic networks is the blocking probability, which is the chance of rejection for a given communication request. In wide-area optical networks, the blocking probability depends on two situations in the network. First, a possible lack of available resources on the user path in terms of FSU, thus, a capacity-related blocking probability. We denote this as Capacity Blocking ($\mathcal{CB}$). Second, for a given transmission request, despite the routing strategy, the chosen path may be too long with no regenerator devices available on the path, resulting in a reach-based blocking probability. We called it Reach Blocking ($\mathcal{RB}$). Therefore, the overall blocking probability ($\mathcal{B}$) can be computed as:

$$\mathcal{B} = \mathcal{CB} + \mathcal{RB}. \tag{8}$$

TABLE 5. Simulation parameters.

Parameter	Value
Resource allocation algorithm	Algorithm 1
$\mathcal{BER}_{th}$	10^{-12}, 10^{-9}, 10^{-6}
Topology	NSFNet
Number of connection requests	10^7
Traffic load ($\varrho_{(s,d)}$)	0.1 - 0.9
Number of FSU by link	320 (12.5 GHz by slot)
Bit rates	10, 40, 100, 400, 1000 Gbps
Modulation formats	BPSK, QPSK, 8-QAM, 16-QAM, 32-QAM, 64-QAM
Optical reach	Table 3
Bandwidth (FSU)	Table 4
Regeneration devices per node	0, 3, 5

Some new performance metrics to evaluate the proposed BER-adaptive algorithm and compare it to Fixed BER approaches have been included. To evaluate the proportion of chosen modulation format on the strategies analyzed here, we foresee two possible cases: no-regenerator scenarios and considering one (or more) 3R regenerators per node. In a no-regenerator scenario, evaluating the proportion of modulation format used in the network is a straightforward task. Let $\mathcal{R}$ be the list of successful connection requests made by all the users of the networks, with cardinality R. Then, consider the subset $\mathcal{R}_{\mathcal{M}^j}$, with $\mathcal{R}_{\mathcal{M}^j} \subset \mathcal{R}$, as the subset of request using the j-th modulation format in $\mathcal{M}$, this is $\mathcal{M}^j$, with cardinality $R_{\mathcal{M}^j}$. This definition is applied to all the modulation formats listed in Table 5. Evidently, this leads to the following:

$$R = \sum_{\forall \mathcal{M}^j \in \mathcal{M}} R_{\mathcal{M}^j}. \tag{9}$$

Then, to compute the proportion of modulation format used in the network, we compute:

$$PP_{\mathcal{M}^j} = \frac{R_{\mathcal{M}^j}}{R}. \tag{10}$$

On the other hand, in a scenario with 3R regenerator devices installed on some network nodes, some user request may use a given modulation format for the first segment of the path, and a different one on the remaining segment. Then, to accurately assess the proportion of modulation format used in the network, we do as follows.

Let H_r be the length on the path used by the r-th request measured as the number of links, and $H_r(\mathcal{M}^j)$ be the number of links of the r-th request using the $\mathcal{M}^j$. Then, to compute the proportion of the chosen modulation level in the network, we compute:

$$PP_{\mathcal{M}^j} = \frac{\sum_{\forall r \in \mathcal{R}_{\mathcal{M}^j}} \frac{H_r(\mathcal{M}^j)}{H_r}}{R}. \tag{11}$$

Remark that this methodology distributes the modulation level used by the user path length measured as the number of links.

Next, the analysis of the results for the proposed BER-Adaptive RMLSA compared to fixed BER RMLSA strategies is presented. First, the case considering nodes without regenerator devices denoted as the *Transparent case* is studied. Second, the case taking into account regenerators on the network nodes, called *Translucent case*, is presented.

B. TRANSPARENT CASE

Here we present the case where no regeneration is taking place on the network focusing on the performance of the strategies in a transparent case.

Figure 4 presents the results of the BER-Adaptive approach and the Fixed BER strategies with 10^{-12}, 10^{-9}, and 10^{-6} BER thresholds with 0 regenerators deployed on the network nodes. The first chart (a) presents the blocking probability $\mathcal{B}$ obtained using the mentioned approaches as a function of the traffic load of the network users. The second one (b) presents the contribution to the blocking probability made by reach ($\mathcal{RB}$) or capacity ($\mathcal{CB}$) blocking for each approach. The third chart (c) presents the proportion of users achieving a BER better than 10^{-12}, 10^{-9}, and 10^{-6} on the BER-Adaptive scheme. Finally, the fourth chart (d) presents the proportion of users using 16QAM, 8QAM, QPSK, and BPSK as a modulation format for all the studied RMLSA strategies. Figure 4 illustrates that in this network, modulation formats with order higher than 16-QAM are not needed since link distances are in general long due to the NSFNet topology.

As shown in Figure 4, the blocking probability $\mathcal{B}$ decreases when the BER threshold is relaxed for fixed BER approaches. In this scenario our proposal obtains similar blocking probability compared to the approach with a fixed BER of 10^{-6}. For a traffic load of 0.3, blocking probabilities of $1.14 \cdot 10^{-2}$ and $7.80 \cdot 10^{-3}$ were obtained for the proposed method and the fixed BER of 10^{-6} approach, respectively. These results can be explained since strict BER thresholds, such as BER 10^{-9} and 10^{-12}, are mainly blocked by reach. This occurs because those QoT thresholds are too strict for the users to achieve communication in the NSFNet network, see MAR in Table 3. Our BER-Adaptive proposal performs similar to the BER 10^{-6} strategy in terms of reach blocking, but the capacity blocking is a slightly higher, as exemplified in Figure 4 chart b), for a traffic load of 0.3 ($\mathcal{CB} = 1.34 \cdot 10^{-3}$ and $\mathcal{CB} = 1.11 \cdot 10^{-3}$ for BER-Adaptive and BER 10^{-6} strategies, respectively).

The difference between BER-Adaptive and BER 10^{-6} strategies can be understood from Figure 4 charts c) and d). Our approach ensures approximately a 57% transmissions with BER 10^{-12} or better, and a 14% extra with 10^{-9} or better, however, BER-Adaptive performs more transmissions using BPSK compared to the fixed BER 10^{-6}. This situation shows that users require more capacity to transmit on the network since BPSK demands more FSU than any other modulation level for a fixed transmission rate.

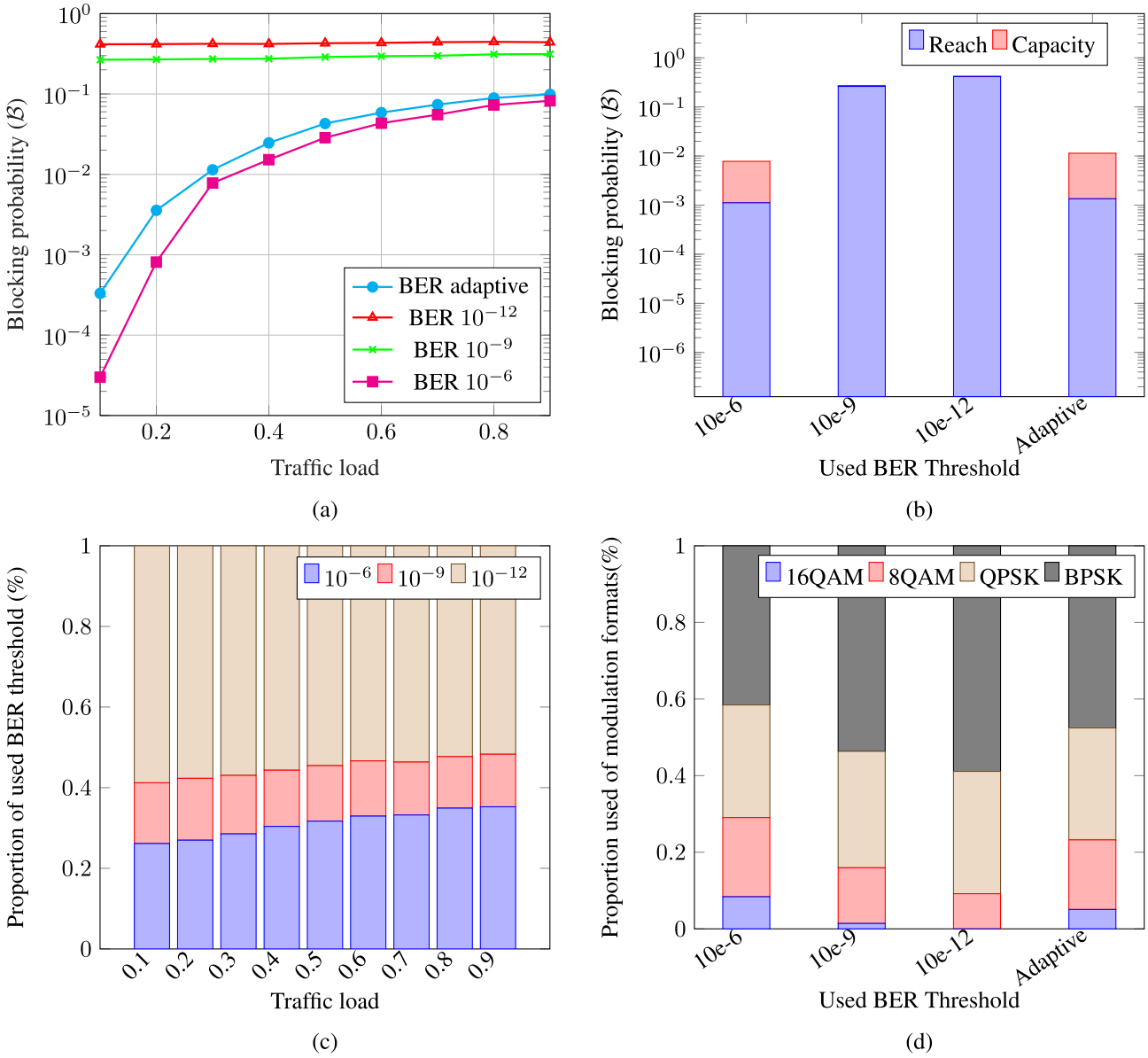

FIGURE 4. Results obtained for 0 regenerators per node case. (a) Blocking probability as function of the user's traffic load. (b) Different contributions of blocked connection requirements due to reach or capacity considering a traffic load equal to 0.3. (c) Proportion of different BER threshold used in the Adaptive algorithm. (d) Proportion of different modulation formats used for the studied algorithms considering a traffic load of 0.3.

This conclusion explains the higher capacity blocking probability of the BER-Adaptive scheme versus the BER 10^{-6}. These results are explained since the BER-Adaptive algorithm prioritizes a better QoT over the bandwidth efficiency of the modulation format.

C. TRANSLUCENT CASE

In this subsection, we present the general case where several regeneration devices are deployed on the network nodes.

Figure 5 shows the outcomes of the BER-Adaptive approach and the Fixed BER strategies with 10^{-12}, 10^{-9}, and 10^{-6} BER thresholds considering 3 regenerators per node. The first chart (a) illustrates the blocking probability $\mathcal{B}$ obtained by the previous strategies as a function of the user's mean traffic load. The second chart (b) presents the contribution to the blocking probability made by reach ($\mathcal{RB}$) or capacity ($\mathcal{CB}$) blocking to the approaches analyzed here. The third chart (c) shows the proportion of users achieving a BER better than 10^{-12}, 10^{-9}, and 10^{-6} on our proposal. The last chart (d) presents the proportion of users using 16QAM, 8QAM, QPSK, and BPSK as a modulation level on the RMLSA schemes.

Similarly, Figure 6 illustrates the results of the BER-Adaptive and Fixed BER strategies with 10^{-12}, 10^{-9}, and 10^{-6} BER thresholds considering 5 regenerators per network node, with the same charts as the previous Figure.

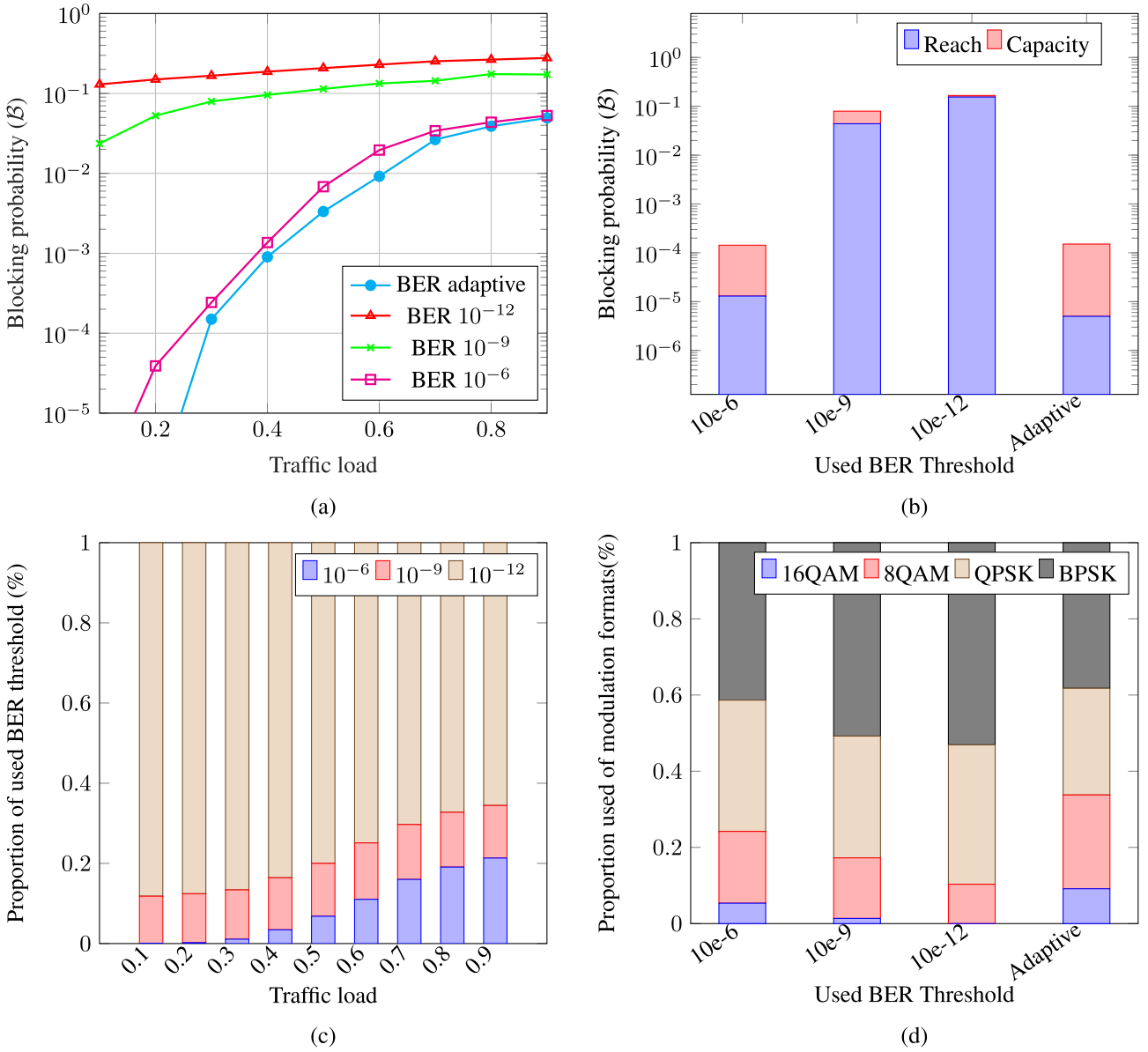

FIGURE 5. Results obtained for 3 regenerators per node case. (a) Blocking probability as function of the user's traffic load. (b) Different contributions of blocked connection requirements due to reach or capacity considering a traffic load equal to 0.3. (c) Proportion of different BER threshold used in the Adaptive algorithm. (d) Proportion of different modulation formats used for the studied algorithms considering a traffic load of 0.3.

First of all, we can contrast the a) charts from Figures 4, 5, and 6 and visualize that deploying regenerators decreases the blocking probability. For instance, Table 6 displays the blocking probability achieved by our BER-Adaptive proposal and the fixed BER methods with 0, 3, and 5 regenerators per node, for a standard value of traffic load ($\varrho = 0.3$ [4]). As displayed in Table 6, despite the method analyzed, the blocking probability decreases when regenerators are added. This situation can be explained since regenerator devices allow to increase the number of users reaching their destinations, thus decreasing the reach blocking probability ($\mathcal{RB}$). Also, these devices allow users to choose a more complex modulation level since it is easier to reach their destination nodes, thus demanding in general less capacity in terms of FSU, and therefore decreasing the capacity blocking probability ($\mathcal{CB}$).

On another note, in both Figures 5 and 6, we can see that, again, on relaxing the BER thresholds, the blocking probability decreases on the fixed BER techniques. In Figure 5, the BER-Adaptive proposal performs slightly better than the fixed BER 10^{-6} strategy. As a matter of fact, in Figure 6, we can see that the blocking probability decreases even more for the BER-Adaptive method. This behavior can be attributed mainly to the reduction of $\mathcal{RB}$, as seen in chart b) in Figures 5 and 6. Additionally, in both figures, the blocking probability for BER 10^{-9} and BER 10^{-12} strategies are primarily due to the reach blocking probability despite the use

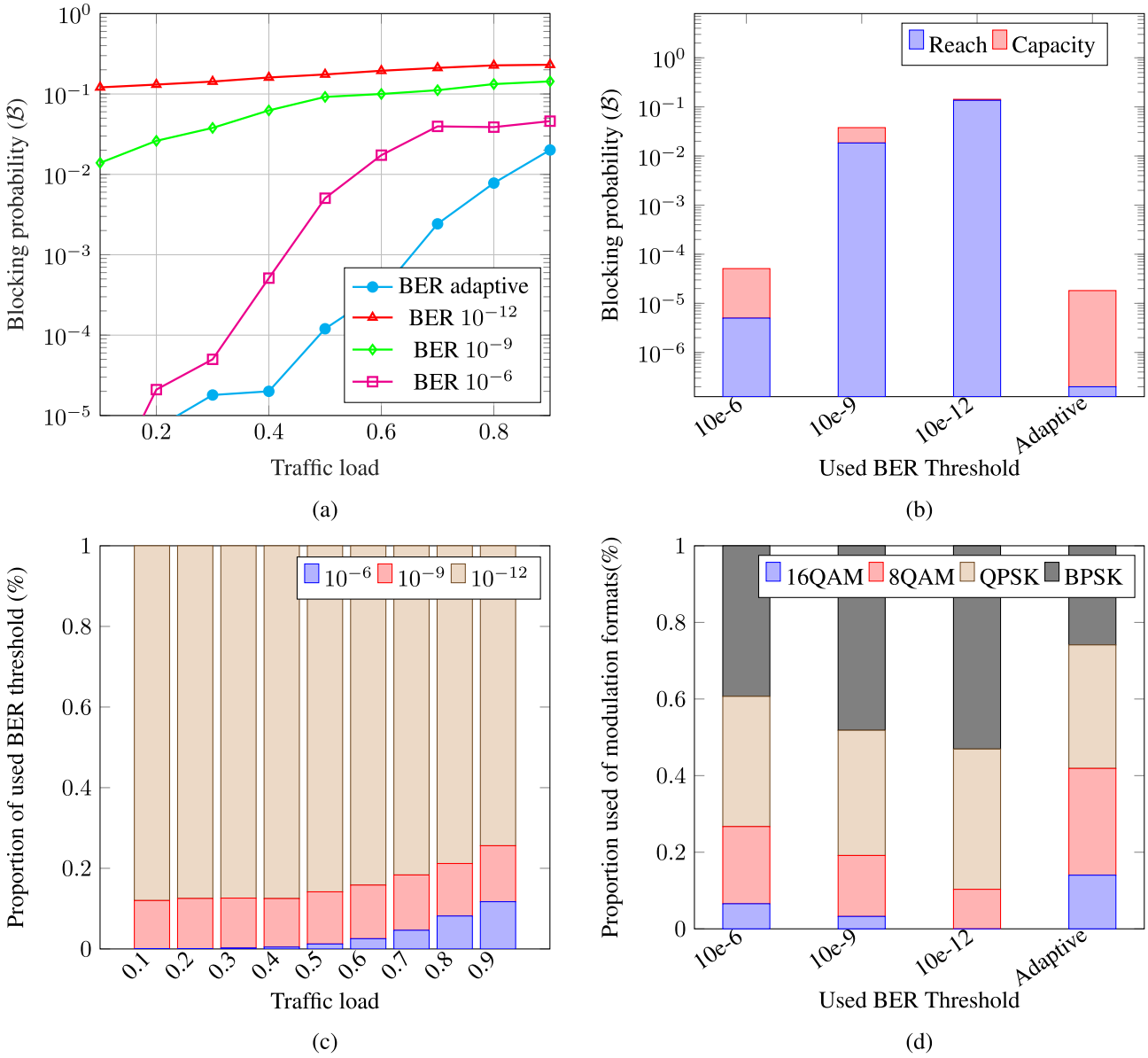

FIGURE 6. Results obtained for 5 regenerators per node case. (a) Blocking probability as function of the user's traffic load. (b) Different contributions of blocked connection requirements due to reach or capacity considering a traffic load equal to 0.3. (c) Proportion of different BER threshold used in the Adaptive algorithm. (d) Proportion of different modulation formats used for the studied algorithms considering a traffic load of 0.3.

of regeneration devices in the network nodes. As illustrated in chart c) from Figures 5 and 6, for the BER-Adaptive case, roughly 80% of the connections guarantee a BER of 10^{-12}, and almost 100% of them ensure a BER of 10^{-9} for a traffic load value of $\varrho = 0.3$. Consequently, the BER-Adaptive strategy achieves a high quality of transmission with low blocking probability.

Comparing the BER-Adaptive and BER 10^{-6} approaches in Figure 5 chart b), we can see that they perform similarly in a traffic load equal to 0.3. However, the blocking situations differ since the BER-Adaptive proposal incurs in less reach blocking and more capacity blocking than fixed BER 10^{-6} technique. Figure 6 shows even more differences between the BER-Adaptive strategy compared to fixed BER threshold methods. The blocking probability of our proposal is considerably lower than any other approach, even compared to the BER 10^{-6} approach.

To understand these differences, we add Tables 7 and 8, illustrating the number of transparent and translucent connections achieved by the BER-Adaptive and BER 10^{-6} techniques using 3 and 5 regenerator devices per node, respectively. The main difference is the number of transparent connections established. The fixed BER 10^{-6} approach establishes $9.92 \cdot 10^6$ (99.23%) and $9.79 \cdot 10^6$ (97.94%) transparent successful connections using 3 and 5 regenerator devices per node. This conduct occurs due to BER 10^{-6}

TABLE 6. Blocking Probability obtained by BER-Adaptive and fixed BER approaches with 0, 3 and 5 regenerators per node for a traffic load of $\varrho = 0.3$.

Method	0 Regs	3 Regs	5 Regs
BER-Adaptive	$1.14 \cdot 10^{-2}$	$1.50 \cdot 10^{-4}$	$1.80 \cdot 10^{-5}$
BER 10^{-6}	$7.80 \cdot 10^{-3}$	$2.43 \cdot 10^{-4}$	$5.00 \cdot 10^{-5}$
BER 10^{-9}	$2.72 \cdot 10^{-1}$	$7.95 \cdot 10^{-2}$	$3.78 \cdot 10^{-2}$
BER 10^{-12}	$4.20 \cdot 10^{-1}$	$1.66 \cdot 10^{-1}$	$1.42 \cdot 10^{-1}$

TABLE 7. The number of established connections for each available route k, using 3 regenerators by node.

Path	BER-Adaptive		BER 10^{-6}	
used (k)	Transparent	Translucent	Transparent	Translucent
1	$5.78 \cdot 10^6$	$3.61 \cdot 10^6$	$9.79 \cdot 10^6$	$6.26 \cdot 10^4$
2	$5.84 \cdot 10^4$	$4.15 \cdot 10^5$	$1.23 \cdot 10^5$	$1.09 \cdot 10^4$
3	0	$1.24 \cdot 10^5$	$4.00 \cdot 10^3$	0

technique defines a very relaxed BER threshold, which can be achieved by almost every connection request, but the largest ones (in km). Therefore, the BER 10^{-6} strategy has low regenerator device usage.

On the other hand, the BER-Adaptive approach establishes $5.84 \cdot 10^6$ (58.4%) and $3.72 \cdot 10^6$ (37.27%) transparent connections with 3 and 5 regenerator devices per node, respectively (as seen in Table 7 and 8). This performance is justified by the nature of the BER-Adaptive algorithm, which prioritizes the use of a strict BER threshold, in order to maintain a high quality of transmission (QoT), relying more on the use of regenerator devices (it successfully communicates $4.14 \cdot 10^6$ and $6.26 \cdot 10^6$ translucent connections for 3 and 5 regenerators per device cases). Only when no regeneration devices are available on the selected path, BER-Adaptive tries to establish communication using a less strict BER threshold. Consequently, high regenerator usage decreases the reach blocking probability and increases the use of highly efficient modulation formats. In Figures 5 and 6 chart d), we can conclude that, while extending the number of regenerator devices, the number of connections using complex modulation increases. For instance, a 14% of connections use 16QAM modulation format with 5 regenerators per device, compared with a 9% for the 3 regenerators per node case, and a 5% in the transparent case. Nevertheless, for long connections, the preference for a strict BER threshold restricts the modulation formats available to the ones with low efficiency. Then, these users demand a larger number of FSU, increasing the capacity blocking probability.

V. CONCLUSION

In this work, we present a novel BER-adaptive solution to solve the routing, modulation format, and spectrum assignment (RMLSA) problem for wide-area elastic optical networks. Our proposal customizes the bit-error-rate (BER) threshold adaptively, increasing the chance to transmit -even in long-distance connections- with the strictest BER and the most efficient modulation format possible. However, in wide-area networks, the accumulation of physical layer impairments (PLI) limits the possibility of achieving transparent transmissions. Then, we consider the use of one 3R regeneration device per connection request.

TABLE 8. The number of established connections for each available route k, using 5 regenerators by node.

Path	BER-Adaptive		BER 10^{-6}	
used (k)	Transparent	Translucent	Transparent	Translucent
1	$3.72 \cdot 10^6$	$5.41 \cdot 10^6$	$9.66 \cdot 10^6$	$1.92 \cdot 10^5$
2	0	$7.48 \cdot 10^5$	$1.24 \cdot 10^5$	$1.19 \cdot 10^4$
3	0	$1.10 \cdot 10^5$	$3.30 \cdot 10^3$	0

Numerical examples compare the BER-Adaptive strategy with standard fixed BER threshold criteria, using 10^{-6}, 10^{-9}, and 10^{-12} BER values. In a nutshell, our proposal achieves similar (and sometimes better) blocking probability than the more relaxed BER threshold value (10^{-6}), but ensures a much higher quality of transmissions to most of the connection request. For instance, in a 0 regenerator scenario, 60% and 75% of the connection requests guarantee a BER of 10^{-12} and 10^{-9}, respectively. On the other hand, with regeneration devices, 90% and 99% of the connection request guarantee a BER of 10^{-12} and 10^{-9}, respectively.

The results show the importance of using 3R regeneration devices, and to adjust the BER thresholds adaptively to maximize the successful connection rate in wide-area elastic optical networks. This way, we can find a balance between the quality level of each transmission request and the quality of service offered to each network user.

REFERENCES

[1] V. López and L. Velasco, Eds., *Elastic Optical Networks*. Cham, Switzerland: Springer, 2016.

[2] H. Waldman, "The impending optical network capacity crunch," in *Proc. SBFoton Conf.*, 2018, pp. 1–4.

[3] A. D. Ellis, N. M. Suibhne, D. Saad, and D. N. Payne, "Communication networks beyond the capacity crunch," *Phil. Trans. Roy. Soc. A, Math., Phys. Eng. Sci.*, vol. 374, no. 2062, Mar. 2016, Art. no. 20150191.

[4] A. Saleh and J. Simmons, "Technology and architecture to enable the explosive growth of the Internet," *IEEE Commun. Mag.*, vol. 49, no. 1, pp. 126–132, Jan. 2011.

[5] R. Zhu, S. Li, P. Wang, Y. Tan, and J. Yuan, "Gradual migration of co-existing fixed/flexible optical networks for cloud-fog computing," *IEEE Access*, vol. 8, pp. 50637–50647, 2020.

[6] I. B. Villy, *Teletraffic Engineering Handbook*. Lyngby, Denmark: ITU-D SG, 2002.

[7] O. Gerstel, M. Jinno, A. Lord, and S. J. Yoo, "Elastic optical networking: A new dawn for the optical layer?" *IEEE Commun. Mag.*, vol. 50, no. 2, pp. s12–s20, Feb. 2012.

[8] J. Yuan, R. Zhu, Y. Zhao, Q. Zhang, X. Li, D. Zhang, and A. Samuel, "A spectrum assignment algorithm in elastic optical network with minimum sum of weighted resource reductions in all associated paths," *J. Lightw. Technol.*, vol. 37, no. 21, pp. 5583–5592, Nov. 1, 2019.

[9] J. Yuan, Y. Fu, R. Zhu, X. Li, Q. Zhang, J. Zhang, and A. Samuel, "A constrained-lower-indexed-block spectrum assignment policy in elastic optical networks," *Opt. Switching Netw.*, vol. 33, pp. 25–33, Jul. 2019.

[10] X. Luo, Y. Zhao, X. Chen, L. Wang, M. Zhang, J. Zhang, Y. Ji, H. Wang, and T. Wang, "Manycast routing, modulation level and spectrum assignment over elastic optical networks," *Opt. Fiber Technol.*, vol. 36, pp. 317–326, Jul. 2017.
[11] A. Fontinele, I. Santos, J. N. Neto, D. R. Campelo, and A. Soares, "An efficient IA-RMLSA algorithm for transparent elastic optical networks," *Comput. Netw.*, vol. 118, pp. 1–14, May 2017.
[12] X. Li, S. Huang, S. Yin, B. Guo, Y. Zhao, J. Zhang, M. Zhang, and W. Gu, "Distance-adaptive routing, modulation level and spectrum allocation (RMLSA) in k-node (edge) content connected elastic optical datacenter networks," in *Proc. 21st Optoelectron. Commun. Conf. (OECC), Held Jointly With Int. Conf. Photon. Switching (PS)*, 2016, pp. 1–3.
[13] T. Hashimoto, K. I. Baba, and S. Simojo, "A study on routing, modulation level, and spectrum allocation algorithms for elastic optical path networks," in *Proc. 3rd Int. Conf. Photon. (ICP)*, 2012. pp. 395–399.
[14] M. Klinkowski, K. Walkowiak, and M. Jaworski, "Off-line algorithms for routing, modulation level, and spectrum assignment in elastic optical networks," in *Proc. 13th Int. Conf. Transparent Opt. Netw.*, Jun. 2011, pp. 1–6.
[15] K. Wen, Y. Yin, D. J. Geisler, S. Chang, and S. J. B. Yoo, "Dynamic on-demand lightpath provisioning using spectral defragmentation in flexible bandwidth networks," in *Proc. 37th Eur. Conf. Exhib. Opt. Commun.*, Washington, DC, USA, vol. 1, 2011, pp. 1–3.
[16] T. Takagi, H. Hasegawa, K. Sato, Y. Sone, B. Kozicki, A. Hirano, and M. Jinno, "Dynamic routing and frequency slot assignment for elastic optical path networks that adopt distance adaptive modulation," in *Proc. Opt. Fiber Commun. Conf./Nat. Fiber Opt. Eng. Conf.*, 2011, pp. 1–3.
[17] V. A. C. Vale and R. C. Almeida, Jr., "Power, routing, modulation level and spectrum assignment in all-optical and elastic networks," *Opt. Switching Netw.*, vol. 32, pp. 14–24, Apr. 2019.
[18] A. Fallahpour, H. Beyranvand, S. A. Nezamalhosseini, and J. A. Salehi, "Energy efficient routing and spectrum assignment with regenerator placement in elastic optical networks," *J. Lightw. Technol.*, vol. 32, no. 10, pp. 2019–2027, May 15, 2014.
[19] H. Beyranvand and J. A. Salehi, "A quality-of-transmission aware dynamic routing and spectrum assignment scheme for future elastic optical networks," *J. Lightw. Technol.*, vol. 31, no. 18, pp. 3043–3054, Sep. 15, 2013.
[20] P. M. Moura, R. A. Scaraficci, and N. L. S. D. Fonseca, "Algorithm for energy efficient routing, modulation and spectrum assignment," in *Proc. IEEE Int. Conf. Commun. (ICC)*, Jun. 2015, pp. 5961–5966.
[21] M. Aibin and K. Walkowiak, "Adaptive modulation and regenerator-aware dynamic routing algorithm in elastic optical networks," in *Proc. IEEE Int. Conf. Commun. (ICC)*, London, U.K., Jun. 2015, pp. 5138–5143.
[22] D. A. R. Chaves, E. F. da Silva, C. J. A. Bastos-Filho, H. A. Pereira, and R. C. Almeida, "Heuristic algorithms for regenerator assignment in dynamic translucent elastic optical networks," in *Proc. 17th Int. Conf. Transparent Opt. Netw. (ICTON)*, Budapest, Hungary, Jul. 2015, pp. 1–4.
[23] D. A. R. Chaves, M. A. Cavalcante, H. A. Pereira, and R. C. Almeida, "A case study of regenerator placement and regenerator assignment in dynamic translucent elastic optical networks," in *Proc. 18th Int. Conf. Transparent Opt. Netw. (ICTON)*, Trento, Italy, Jul. 2016, pp. 1–4.
[24] Ì. Brasileiro, J. Valdemir, and A. Soares, "Regenerator assignment with circuit invigorating," *Opt. Switching Netw.*, vol. 34, pp. 58–66, Nov. 2019.
[25] I. B. Brasileiro, A. C. B. Soares, and J. V. D. Reis, "Planning and evaluation of translucent elastic optical networks in terms of cost-benefit," in *Proc. 19th Int. Conf. Transparent Opt. Netw. (ICTON)*, Girona, Spain, Jul. 2017, pp. 1–4.
[26] D. Eppstein, "Finding the K shortest paths," *SIAM J. Comput.*, vol. 28, no. 2, pp. 652–673, 1999.
[27] B. C. Chatterjee, N. Sarma, and E. Oki, "Routing and spectrum allocation in elastic optical networks: A tutorial," *IEEE Commun. Surveys Tuts.*, vol. 17, no. 3, pp. 1776–1800, 3rd Quart., 2015.
[28] P. Poggiolini, G. Bosco, A. Carena, V. Curri, Y. Jiang, and F. Forghieri, "The GN-model of fiber non-linear propagation and its applications," *J. Lightw. Technol.*, vol. 32, no. 4, pp. 694–721, Feb. 15, 2014.
[29] P. Poggiolini, G. Bosco, A. Carena, V. Curri, Y. Jiang, and F. Forghieri, "A detailed analytical derivation of the GN model of non-linear interference in coherent optical transmission systems," 2012, *arXiv:1209.0394*. [Online]. Available: http://arxiv.org/abs/1209.0394
[30] R.-J. Essiambre, G. Kramer, P. J. Winzer, G. J. Foschini, and B. Goebel, "Capacity limits of optical fiber networks," *J. Lightw. Technol.*, vol. 28, no. 4, pp. 662–701, Feb. 15, 2010.
[31] D. J. Ives, P. Bayvel, and S. J. Savory, "Adapting transmitter power and modulation format to improve optical network performance utilizing the Gaussian noise model of nonlinear impairments," *J. Lightw. Technol.*, vol. 32, no. 21, pp. 4087–4096, Nov. 1, 2014.
[32] *Characteristics of a Single-Mode Optical Fiber and Cable*, document ITU G.652, 2016. Accessed: Jun. 21, 2020.
[33] J. Proakis, *Digital Communication*. New York, NY, USA: McGraw-Hill, 2000.

FELIPE IGNACIO CALDERÓN received the B.Sc. degree in electronic engineering from the Pontificia Universidad Católica de Valparaíso (PUCV), Chile, in 2020. His current interests include optical networking, fiber optic communication systems, and optimization and machine learning.

ASTRID LOZADA received the bachelor's degree in telecommunication engineering from the Universidad Nacional Experimental Politécnica de la Fuerza Armada, Venezuela, in 2012. She is currently pursuing the master's degree in electronic engineering with the Universidad Técnica Federico Santa María, Valparaíso, Chile.

DANILO BÓRQUEZ-PAREDES received the B.Eng. degree and the professional title in telematics engineering from Universidad Técnica Federico Santa María (UTFSM), Valparaíso, Chile, in 2012, and the Ph.D. degree from Universidad Adolfo Ibañez, in September 2018. He is currently a full-time Professor with the Engineering and Sciences Faculty, Universidad Adolfo Ibañez. His works focus on the dynamic allocation of resources in flexible optical networks, network virtualization, graph theory, and optimization.

RICARDO OLIVARES received the B.Sc. degree in electronic engineering from Universidad Técnica Federico Santa María (UTFSM), Chile, in 1983, and the M.Sc. and D.Sc. degrees in electrical engineering from the Pontificia Universidade Católica do Rio de Janeiro, Brazil, in 1994 and 2001, respectively. He has been with the Department of Electronic Engineering, UTFSM, since 1986, where he has also been the Head of Department, since 2017. His current interests include RF measurements, fiber optic communication systems, fiber optical sensors, and nonlinear fiber optics.

ENRIQUE JAVIER DAVALOS (Member, IEEE) received the degree in electromechanics engineering, the M.Sc. degree in systems engineering, and the Ph.D. degree in computer sciences from the Universidad Nacional de Asunción, Paraguay, in 1987, 2010, and 2018, respectively. He worked at IBM World Trade Corporation as a Global Services Coordinator, from 1987 to 2004, and the Services Representative at PSLine S.A., from 2004 to 2008. Since 2009, he has been a full-time Professor and a Researcher with the Facultad Politécnica, Universidad Nacional de Asunción. He is the author of 20 articles. His research interests include optical networks, network security, and multi-objective optimization.

GABRIEL SAAVEDRA (Member, IEEE) received the B.Eng. degree in telecommunication engineering and the M.Sc. degree from the Universidad de Concepción, Chile, in 2013 and 2014, respectively, and the Ph.D. degree from University College London (UCL), London, U.K., in 2019. He is currently an Associate Professor with the Universidad de Concepción. His research interests are nonlinear fiber effects, nonlinear compensation methods, and digital signal processing for optical communications.

NICOLÁS JARA received the B.Sc. degree in telematics engineering and the M.Sc. degree in telematics engineering from Universidad Técnica Federico Santa María (UTFSM), Chile, in 2010, and the Ph.D. degree on a double graduation program from the Université de Rennes I, France, and UTFSM, in 2017 and 2018, respectively. He is currently an Assistant Professor with the Department of Electronics, UTFSM. His current research interests include optical networks design, networks performability, and simulation techniques.

ARIEL LEIVA (Member, IEEE) received the B.Sc. degree in electronic engineering and the M.Sc. degree in electrical engineering from the Pontificia Universidad Católica de Valparaíso (PUCV), Chile, in 2003 and 2007, respectively, and the Ph.D. degree from Universidad Técnica Federico Santa María, Valparaíso, Chile, in 2013. He is currently a Lecturer with PUCV. His current interests include fiber optic communication systems and optical networking.